Structure and Mechanical Properties of the Compositions of Polyisocyanurate Polymers with Low Molecular Weight Rubbers

ANDREI A. ASKADSKII,* ALEXANDER E. SHVORAK, TSYLIA M. FRENKEL, TATYANA M. BABTSCHINITZER, CAPITOLINA A. BYCHKO, OLEG V. KOVRIGA, VIATSCHESLAV A. PANKRATOV, and A. VARADA RAJULU†

Institute of Organoelement Compounds, Russian Academy of Sciences, 28, Vavilov St., Moscow, V-334, Russia

SYNOPSIS

The structure and properties of the compositions of polyisocyanurates modified with low molecular weight rubber networks have been investigated by means of dynamical mechanical analysis (DMA), electron microscopy, and stress-relaxation experiments. The network compositions consist of two different polymeric networks. The first component (macrodiisocyanate based on low molecular weight polybutadiene or copolymers of tetrahydrofuran and propylene oxide) has bulky cross-linked points connected by short flexible chains. The second component (diphenylmethanediisocyanate) also has bulky cross-linked points of the same structure, but the linear fragments between them in this case are very small and rigid. These compositions result in the formation of the heterophase system. As a result, transparent samples were prepared, which differ from the mechanical properties of both the glassy and rubbery polymers. These materials have a modulus of elasticity (from 10^3 to 10 MPa) that is usual for the transition zone between the glassy and rubbery states; nevertheless, these materials show elastic (and not viscoelastic) properties. For the materials investigated, the modulus is decreased not more than 10 times in the wide temperature interval from 200 to 500 K. A new state of the polymer, which differs from both the glassy and rubbery states, has been identified in the present case. © 1995 John Wiley & Sons, Inc.

INTRODUCTION

Modification of rigid polymer networks with reactive rubber oligomers permits one to increase the impact resistance of polymers significantly. Thermodynamical analysis of phase transitions in different polymers, e.g., in epoxy–rubber systems,[1] shows that the thermodynamical compatibility of the components varies depending on the content of rubber during the polymerization process and, hence, phase separation occurs. The investigation of the rupture mechanics in the epoxy–rubber systems[2-5] reveal that the rupture effective energy depends on the rubbery phase particles' dimensions, which, in turn, depend on the compatibility of the components. The smallest dimensions of rubber particles (about 1000 Å) have been reported in compositions with polar rubbers (e.g., butadieneacrylonytrile).[2-5] Thus, one can change the phase separation and properties of a copolymer by changing the composition of the rubber oligomers.

It is known that usual polymer networks in the glassy state have an elastic modulus about 2–3 $\times 10^3$ MPa, which is almost independent of the network's chemical structure. After the glass transition, the rubbery polymer has a modulus some orders lower (from 0.1 to 30–50 MPa for polymers with various cross-linked points density). Such a decrease in the polymer's modulus occurs in a very narrow temperature interval (20–30°C).

It is also known that for both glassy and rubbery states a relaxation stress comes quickly to the quasi-equilibrium state and the equilibrium stress σ_∞ for them is finite. For polymers in the transition zone, the relaxation process goes very intensively up to $\sigma_\infty \to 0$. For this reason, we will arbitrarily call both

* To whom correspondence should be addressed.

Journal of Applied Polymer Science, Vol. 55, 1173–1183 (1995)
 CCC 0021-8995/95/081173-11

the glassy and rubbery polymers elastic, whereas those in the transition zone, viscoelastic.

The possibility to synthesize the rubbery polymer networks with an elastic modulus, which is higher than for the polymers in rubbery state, has been reported in some recent articles.[6,7] It is necessary to note that the materials described in Refs. 6 and 7 are transparent and do not contain any plastisizers or fillers. Schematic representation of such a structure is shown in Figure 1. It has bulky rigid cross-linked points connected with each other by short and flexible linear chains. The authors[6,7] considered isocyanurate cycles with attached aromatic cycles as the cross-linked points and the polydimethylsiloxane fragments with a few repeating units as flexible chains.

In the present work, the structure and properties of the compositions of polyisocyanurates (derived from aromatic diisocyanate) modified by low molecular weight rubbers have been studied using dynamical mechanical analysis (DMA), electron microscopy, and small-angle X-ray diffraction (SAXD) techniques. The glass transition temperatures of the networks with various compositions and structures were calculated theoretically and compared with the observed values.

EXPERIMENTAL

Diphenylmethandiisocyanate (LMDI) was used as the rigid component, whereas butadiene (M_n = 2000) and low molecular weight copolymers of tetrahydrofurane and propylene oxide (M_n = 1700) was used as the rubber components. The structures [(**1**) and (**2**)] of the rubber components are described below:

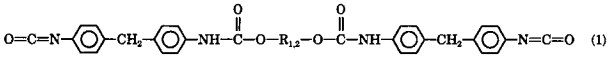

(1)

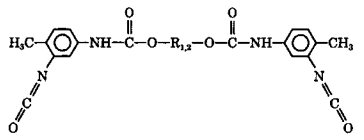

(2)

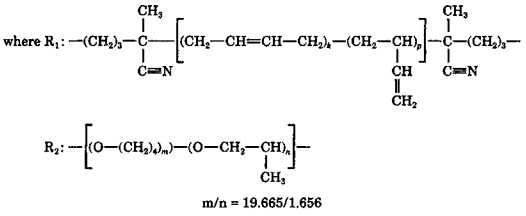

The reactivity of the component with structure (**1**) is equal to LMDI's reactivity, but for rubber (**2**), the polycyclotrimerization rate is lower than that of LMDI polycyclotrimerization due to the screening effect of the methyl group in *ortho* position. The resulting networks [structures (**I**)–(**V**)] due to polycyclotrimerization are presented below:

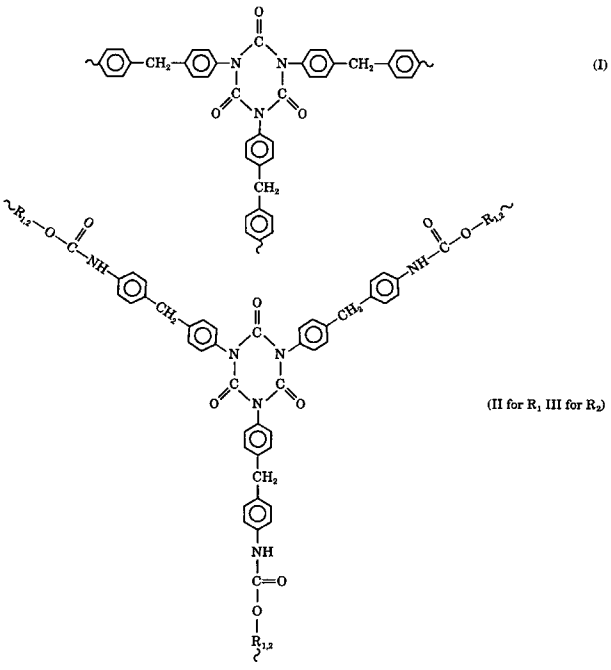

(I)

(II for R_1 III for R_2)

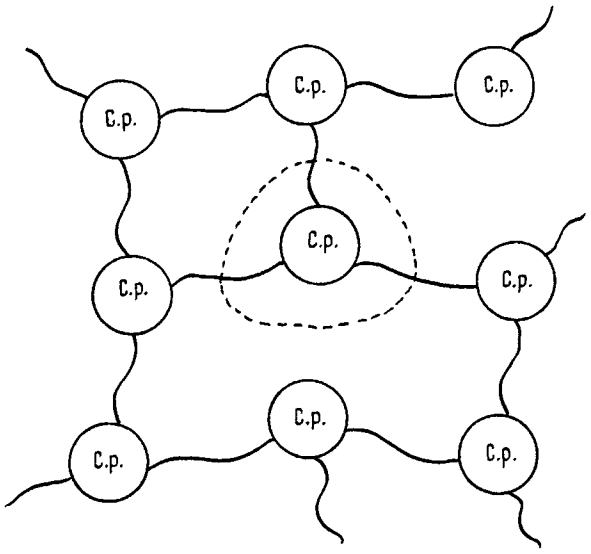

Figure 1 Schematic structure of network with big rigid three functional cross-linked points connected to each other by short and flexible linear chains.

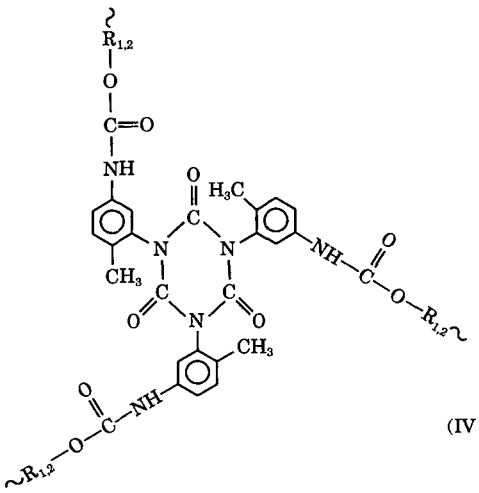

(IV for R_1 V for R_2)

Copolymerization of different networks with different structures (**I–V**) was conducted stage by stage at 120, 150, 180, and 200°C (2 h for every stage) and the catalytical system used was teramine-α-oxide. The investigated compositions are listed in Table I. LMDI and networks (**II**) and (**III**) are transparent, whereas networks (**IV**) and (**V**) are opaque in nature.

The measurements of the storage modulus E' and the loss factor tan δ were conducted with a device described in Ref. 8.

The DMA was carried out under tensile mode vibration and constant tensile stress on the samples taken in the form of strips with the thickness of about 150–200 μm, width of 2 mm, and length of 30 mm. Electron microscope objects are ultrathin sections of the samples (stained by OsO_4). The relaxation measurements were carried out on the rectangular samples ($4 \times 4 \times 6$ mm) under constant strain of 3%. The speed of initial deformation was 1.57%/min.

Table I The List of Investigated Compositions

Composition	Rubbery Phase Content (%)
I/V	0
I/V	19
I/V	28
I/V	39
I/V	44
I/V	100
I/II	21
I/II	30
I/III	28
I/III	43
I/IV	21

RESULTS AND DISCUSSION

Theoretical Calculation of Glass Transition Temperature

The glass transition temperature (T_g) for the five structures shown in the Experimental section were calculated theoretically using eq. (1):[9-10]

$$T_g = \frac{\sum\limits_i \Delta V_i}{\left(\sum\limits_i a_i \Delta V_i + \sum\limits_i b_i\right)_{\text{lin}} + \left(\sum\limits_i K_i \Delta V_i\right)_{C.P.}} \quad (1)$$

where $\sum\limits_i \Delta V_i$ is the van der Waals' volume of the network's repeating fragment (it is shown inside the dashed line in Fig. 1), and a_i, b_i, and k_i are increments that characterize the weak dispersion interactions, specific intermolecular interactions, and chemical bonding energy, respectively.

According to Refs. 9 and 10, the cross-linked point of the network consists of the group of atoms including the first atom of the chain's branching, the neighboring atoms, chemically bound with it, and the closest substituents of these neighboring atoms.

Van der Waals' volumes of the network (**III**)'s cross-linked point and linear chain between the cross-linked points are taken as an example and are calculated below:

$$\left(\sum_i \Delta V_i\right)_{C.P.} = 3\Delta V^*_{C_1} + 3\Delta V_{C_{21}} + 3\Delta V_{O_{134}} + 3\Delta V_{N_{139}}$$

$$\left(\sum_i \Delta V_i\right)_{\text{lin}} = 2 \cdot (8\Delta V_{C_{18}} + 2\Delta V_{C_{19}} + \Delta V_{C_{12}} + \Delta V_{C_{21}} + \Delta V_{C_{64}} + 10\Delta V_{H_{119}} + \Delta V_{H_{122}} + \Delta V_{O_{134}} + \Delta V_{O_{124}} + \Delta V_{N_{140}}) + 1.656(\Delta V_{C_{39}} + \Delta V_{C_{38}} + \Delta V_{C_{13}} + 6\Delta V_{H_{119}} + \Delta V_{O_{124}}) + 19.665(2\Delta V_{C_{39}} + 2\Delta V_{C_{10}} + 8\Delta V_{H_{119}} + \Delta V_{O_{124}})$$

ΔV_i indexes coinside with the atoms' numbers in the table of van der Waals' volumes.[9] Unknown van der Waals' volumes were calculated in this work (they are marked with "*").

The result is

$$\left(\sum_i \Delta V_i\right)_{C.P.} = 98 \text{ Å}^3$$

$$\left(\sum_i \Delta V_i\right)_{\text{lin}} = 2027 \text{ Å}^3$$

Then,

$$\left(\sum_i a_i\Delta V_i\right)_{\text{lin}} = a_C[2(\Delta V_{C_{64}} + 2\Delta V_{C_{19}} + \Delta V_{C_{12}} + \Delta V_{C_{21}} + 8\Delta V_{C_{18}}) + 1.656(\Delta V_{C_{39}} + \Delta V_{C_{38}} + \Delta V_{C_{13}}) + 19.665(2\Delta V_{C_{39}} + 2\Delta V_{C_{10}})] + a_H[2(10\Delta V_{H_{119}} + \Delta V_{H_{122}}) + 1.656 \cdot 6\Delta V_{H_{119}} + 19.665 \cdot 8\Delta V_{H_{119}}] + a_{O_5} \cdot 2\Delta V_{O_{134}} + a_{O,b}(2\Delta V_{O_{124}} + 1.656\Delta V_{O_{124}} + 19.665\Delta V_{O_{124}}) + a_{N,b}2\Delta V_{N_{140}}$$

$$\sum_i b_i = 2b_h + 1.656b_d + 2 \cdot 2b_h$$

$$\left(\sum_i K_i\Delta V_i\right)_{C.P.} = K_C \cdot 3\Delta V_{C_{21}} + K_C^d \cdot 3\Delta V_{C_1}^* + K_O^d \cdot 3\Delta V_{O_{134}} + K_N^d \cdot 3\Delta V_{N_{139}}$$

leading to

$$\left(\sum_i a_i\Delta V_i\right)_{\text{lin}} = 9686 \text{ Å}^3 \text{ K}^{-1} 10^{-3}$$

$$\sum_i b_i = -473 \text{ Å}^3 \text{ K}^{-1} 10^{-3}$$

$$\left(\sum_i K_i\Delta V_i\right)_{C.P.} = 154.7 \text{ Å}^3 \text{ K}^{-1} 10^{-3}$$

Then, these values can be put into eq. (1):

$$T_g = \frac{98 + 1.5 \cdot 2027}{154.7 + (9686 - 473) \cdot 1.5} \cdot 10^3 = 224 \text{ [K]}$$

(Every cross-linked point is three-functional and every linear fragment belongs to two cross-linked points. So, there are 3/2 = 1.5 linear fragments per every cross-linked point.) The results of the same calculations for all of the network structures, described in the Experimental part, are presented at the Table II.

In calculating the glass transition temperature of the networks, it is necessary to take allowance for the fact that any network contains some amount of "dangling chain ends." Although polycyclotrimerization of the given oligomers leads to a high conversion, the presence of free end groups in the resulting network is quite possible. Let us examine the influence of these groups on the glass transition temperature. If we take one branch with a free end group (see Fig. 1), the isocyanurate cycle is not a cross-linked point. Such a cycle will contribute to eq. (1) with increments a_i and b_i and not K_i. Let us calculate the glass transition temperature of network (**II**) for the fragment indicated by a dashed line (Fig. 1). For this fragment,

$$\sum_i \Delta V_i = 2\left(\sum_i \Delta V_i\right)_{\text{lin,II}} + 3\Delta V_{N_{139}} + 3\Delta V_{C_2}^* + 3\Delta V_{O_{134}} = 5614 \text{ Å}^3$$

$$\sum_i a_i\Delta V_i + \sum_i b_i = 2\left(\sum_i a_i\Delta V_i\right)_{\text{lin,II}} + 2\left(\sum_i b_i\right)_{\text{lin,II}} + a_C(3\Delta V_{C_2}^* + 3\Delta V_{C_{21}}) + 3a_{O_5}\Delta V_{O_{134}} + 3a_{N,B}\Delta V_{N_{139}} + 3b_d = 26296 \cdot 10^{-3} \text{ Å}^3 \text{ K}^{-1}$$

By substituting these values in eq. (1), one obtains T_g = 213 K, which is nearly the same as the value for the completely cross-linked network (214 K).

Now let us compare the experimental DMA data with calculated glass transition temperatures from the Table II.

Dynamical Mechanical Analysis

To determine the T_g values experimentally, DMA was carried out on the compositions of polyisocyanurate polymers (modified with rubber oligomers) having different quantities of structure (**I**). Figure

Table II The Initial Data and Calculated Glass Transition Temperatures

Structure	$(\Sigma_i \Delta V_i)_{C.P.}$ (Å^3)	$(\Sigma_i \Delta V_i)_{\text{lin}}$ (Å^3)	$(\Sigma_i a_i\Delta V_i)_{\text{lin}} \times 10^3$ (Å^3 K^{-1})	$\Sigma b_i \times 10^3$ (Å^3 K^{-1})	$(\Sigma_i K_i\Delta V_i) \times 10^3$ (Å^3 K^{-1})	T_g (K)
I	98	151	402	−107	155	518
II	98	2767	10,189	2969	155	214
III	98	2027	9,686	−473	155	224
IV	98	2617	9,869	2956	155	207
V	98	1877	9,320	−478	155	217

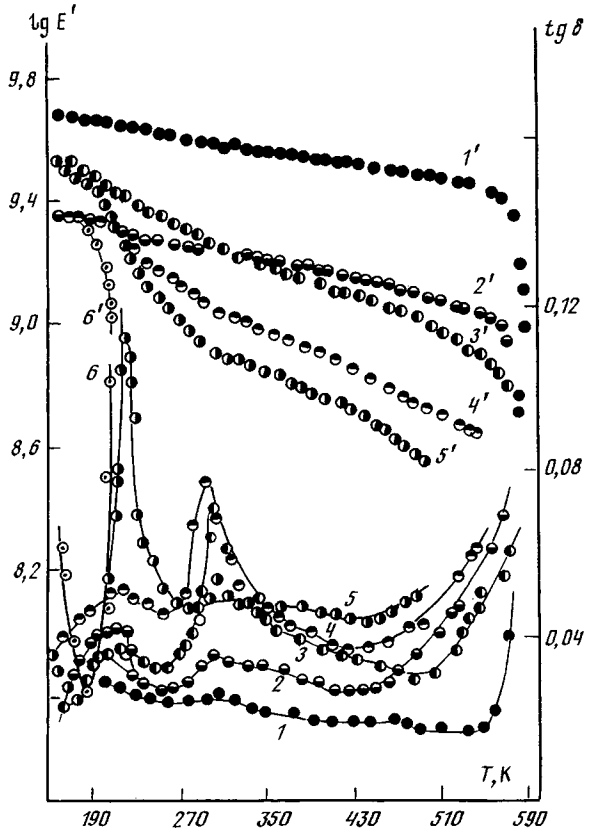

Figure 2 Temperature dependence of (1′–6′) storage modulus E' and (1–6) loss tangent tan δ for the compositions containing structures (**I**) and (**V**). Structure (**V**) content's is (in wt %): 1, 1′, 0; 2, 2′, 19; 3, 3′, 28; 4, 4′, 39; 5, 5′, 44; 6, 6′, 100.

2 shows the temperature dependence of storage modulus E' and loss tangent (tan δ) for networks with structure (**V**) containing various quantities of structure (**I**). From the figure, it is evident that the compositions have some relaxation transitions in the temperature range of 150–560 K. The dependence of E' and tan δ for network (**I**), which does not contain the rubbery component, is typical of high cross-linked glassy polymers. E' decreases slightly with increase of temperature and the tan δ curve does not have any peaks in this temperature region. However, the compositions containing structures (**I**) and (**V**) have a low temperature maximum (in the region 210–220 K) and a wide peak in the 260–340 K region. It is also observed that tan δ rises steeply at high temperature. From the figure, one can see that the temperature corresponding to the low-temperature peak does not change with the flexible component's (**V**) content, though its intensity increases with increasing content of structure (**V**) in the composition. As the observed maxima in the region of 210–220 K is close to the theoretical T_g value of 217 K for structure (**V**), this transition can be attributed to structure (**V**).

The transitions in the temperature range of 260–340 K can probably be related to the interphase. By taking the temperature of the intermediate maximum in the tan δ curve as the glass transition temperature, we can calculate the content of flexible chains and rigid cross-linked points in the interphase using a calculation technique described in Refs. 7 and 10 and eq. (2):

$$T_g = \frac{\alpha_1\left(\sum_i \Delta V_i\right)_1 + (1-\alpha_1)\left(\sum_i \Delta V_i\right)_2}{\alpha_1\left(\sum_i a_i\Delta V_i + \sum b_i + \sum_i K_i\Delta V_i\right)_1 + (1-\alpha_1)\left(\sum_i a_i\Delta V_i + \sum_i b_i + \sum_i K_i\Delta V_i\right)_2} \quad (2)$$

where $(\sum_i \Delta V_i)_1$ and $(\sum_i \Delta V_i)_2$ are van der Waals' volumes of repeating fragments in phases (1) and (2); $(\sum_i a_i\Delta V_i + \sum_i K_i\Delta V_i)_1$ and $(\sum_i a_i\Delta V_i + \sum_i b_i + \sum_i K_i\Delta V_i)_2$ are increment combinations for phases (1) and (2), respectively; and α_1 is the content of rubbery phase (in molar parts). Using eq. (2) it was found that $\alpha_1 = 0.09$, which indicates that there are $\sim$ 10 molar % of the flexible chains and $\sim$ 90 molar % of the rigid cross-linked points (and aromatic cycles, attached to it) in the interphase.

The DMA curves for different compositions of structures (**I**)–(**IV**) and (**I**)–(**II**) are presented in Figure 3. In the case of (**I**)–(**IV**), the low-temperature peak is observed at 208 K, which is in close agreement with the theoretical value of 207 K. (Polybutadiene used contained 77% of structure 1,4-substitution and 23% of structure 1,2-substitution.) Similarly, the low-temperature peak observed for the (**I**)–(**II**) structure is in close agreement with the theoretical T_g value of 214 K. In both cases, the polymers are modified with low molecular weight polybutadiene. Thus, it can be concluded that such compositions with butadiene rubber fragments have the phase structure independent of the reactivity of the initial rubber oligomers and the phase structure in, its turn, does not contribute to the transparency of the material as the compositions with structure (**II**) are transparent, whereas those with structure (**IV**) are opaque.

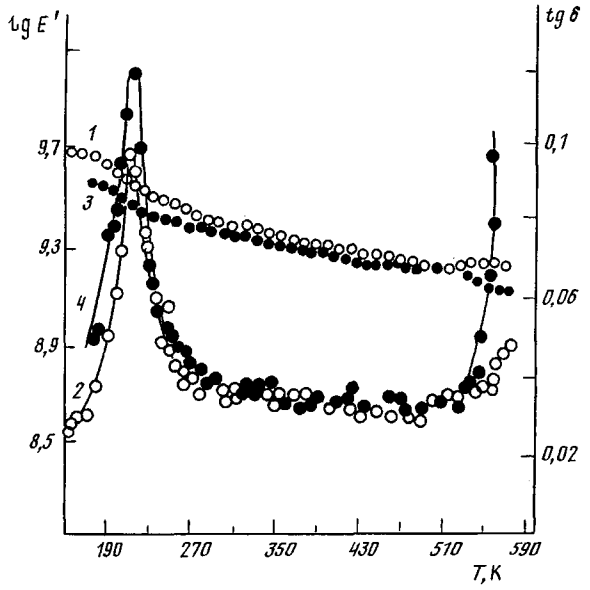

Figure 3 Temperature dependence of (1, 3) E' and (2, 4) tan δ for the compositions (3, 4) with structures (**I**) and (**II**) and (1, 2) with structures (**I**) and (**IV**). For both compositions, the rubbery phase content is ~ 21 wt %.

But for compositions containing rubber fragment R_2, the reactivity of the oligomer's terminal groups influences the phase structure of the composition. It can be seen from Figure 4 that there are two peaks for the composition of structures (**I**) and (**III**), one at 226 K and the other at 452 K. As the theoretical value of T_g for structure (**III**) (224 K) is very close to the temperature corresponding to the first peak, it can be attributed to the T_g of structure (**III**). The other peak at 452 K corresponds to the interphase.

For the structures (**I**)–(**V**), the high-temperature peaks fall above 500 K. As this value is closer to the theoretical T_g value of structure (**I**) (518 K), it can be attributed to structure (**I**).

Comparison of the T_g of the interphases of structures (**III**) and (**V**) (containing the same type of rubber fragment) reveals that the T_g of the interphase of structure (**III**) shifts to a higher temperature, pointing to a change in the composition of the interphase material. Based on the data of Figure 2 (curve 3) and Figure 4 and using eq. (2), it was found that for structure (**V**) the content of rubbery material in the interphase layer $\alpha_1 = 0.11$ and the content of the rigid cross-linked points $\alpha_2 = 0.89$ (in molar fractions). For structure (**III**), $\alpha_1 = 0.02$ and $\alpha_2 = 0.98$. Thus, in the case of structure (**III**), the interphase layer is enriched with the rigid component. It is associated with an increase in the reactivity of oligomers. It can be supposed that for the compositions derived from rubbery oligomers with structure (**2**) having low reactivity (lower than for LMDI) the screening CH_3 group decreases the rate of rubbery oligomer's polycyclotrimerization and so an additional kinetic factor must also be considered. The viscosity of the environment grows during the reaction and probably the formation of the drops with lower viscosity occurs until the gelation takes place. Thus, here, the dimensions of the rubbery phase are bigger, which kinetically show the formation of interphase.

To check this factor of changing the phase dimensions with decrease in the rubbery oligomers' reactivity, a morphological investigation was carried out.

Morphology of Copolymers

The morphology of copolymers of LMDI and tetrahydrofuran/propylene oxide rubber [structures (**III**) and (**V**)] have been studied earlier.[11] So, in this work, only the morphology of the copolymers of LMDI and butadiene rubber (20 wt %) with structures (**II**) and (**IV**) were investigated by small-angle X-ray diffraction (SAXD) and transmission electron microscopy of thin sections stained by OsO_4 vapor. For both the transparent and opaque samples, the weak isotropic reflex with Bragg spacing of 150 Å was observed. This is a typical feature of microphase separation in block copolymers.[12] The SAXD data are consistent with the micrographs that are shown on Figure 5(a). Only the microphase sepa-

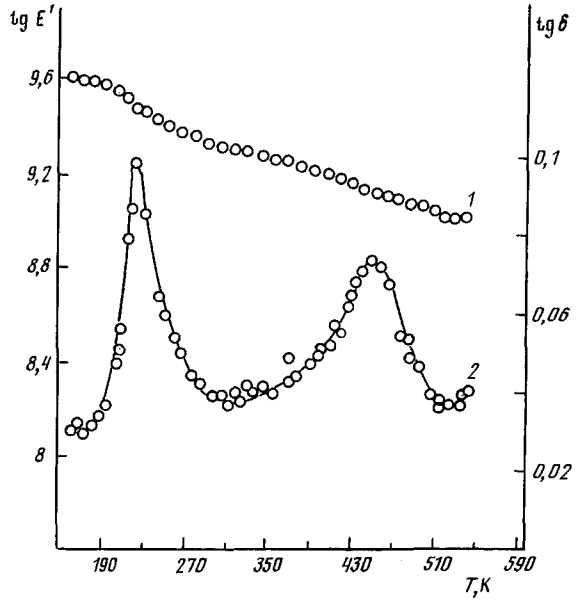

Figure 4 Temperature dependence of (1) E' and (2) tan δ for the composition with structures (**I**) and (**III**), containing ~ 28 wt % of the rubbery phase.

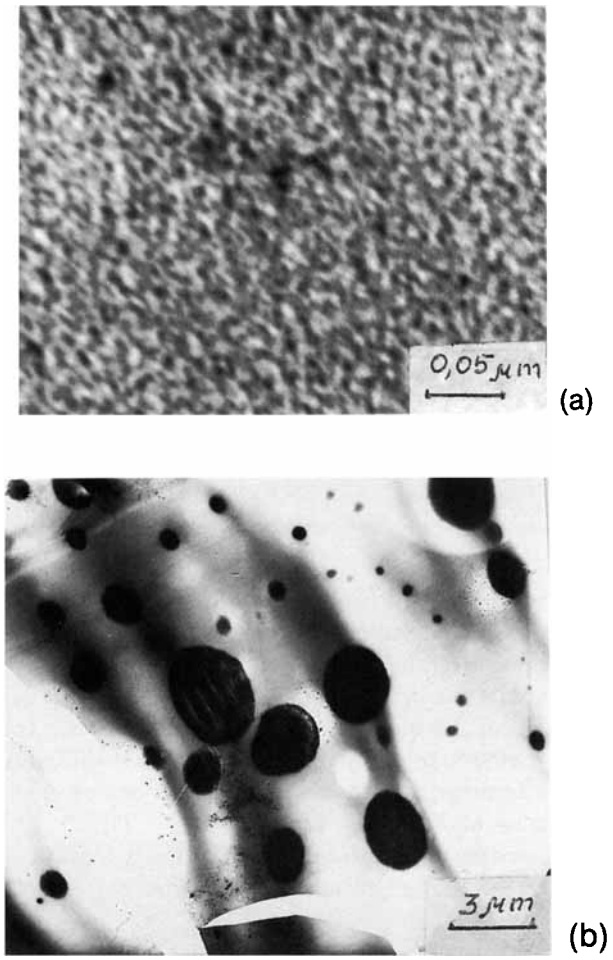

Figure 5 Electron micrographs of the compositions with structures (a) (**I**) and (b) (**I**) and (**IV**).

ration was observed in the transparent material. In the opaque one, electron microscopy reveals not only the microphase separation, but the blend type morphology as well [Fig. 5(b)]. The inclusions are 0.2–10 μm in diameter and have bimodal dimensional distribution. Thus, the morphological investigation confirms the supposition concerning the origin of the transparency of the compositions and shows that the morphology of the samples depends not only on the thermodynamical incompatibility of the copolymer fragments but also on the relative reactivity.

Relaxation Properties of Rubber-modified Isocyanurate Networks

The heterophase structure of these networks results in the unusual mechanical properties depending on compositions. Preliminary analysis shows that at room temperature these materials have an elastic modulus usual for polymers in the transition zone from the glassy to rubbery state and the value of this modulus depends on the network's composition. However, their properties differ very much from that of usual viscoelastic materials in the transition zone.

To analyze the specific features of the relaxation behavior of the materials under study, stress-relaxation experiments[13] were carried out in a wide temperature region. The relaxation curve for the composition of networks (**I**) and (**II**) containing 30% of the rubbery phase is shown on Figure 6 (curve 1). Similar types of curves were observed for all the compositions under consideration in a wide temperature region. For the sake of comparison, the relaxation curve for the usual viscoelastic material, e.g., bisphenol A-based epoxy resin with a lengthened chain, is also presented in the same figure (curve 2). The initial modulii for both samples are equal (the initial modulus E_0 is equal to σ_0/ε_0, where σ_0 is the initial stress in the sample at the final moment of deformation process, and ε_0, the final deformation) and it is clear from Figure 6 that the composition of networks (**I**) and (**II**) as well as composition based on the epoxy resin comes quickly to the quasi-equilibrium state, which is characterized by very small changes of stress with the time, but in the case of compositions (**I**) and (**II**), the equilibrium modulus is finite. So, these materials have the same relaxational behavior as that of glassy polymers, although their modulus is significantly lower. For the epoxy resin mentioned above, the equilibrium modulus is equal to 0.

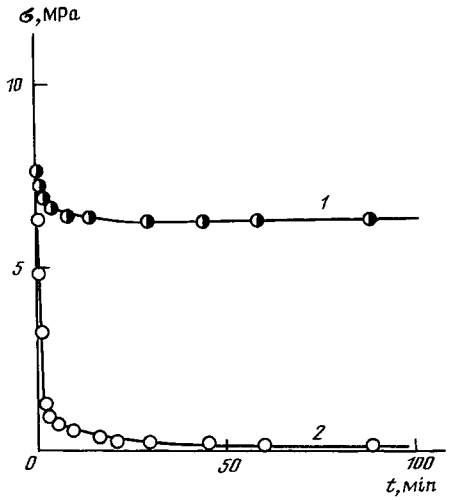

Figure 6 Relaxation curve (1) for the composition of networks (**I**) and (**II**) containing 30% of the rubbery phase and (2) for usual viscoelastic material: bisphenol A-based epoxy resin with a lengthened chain.

The approximation of the relaxation curves is carried out using new memory functions proposed by Askadskii.[14] It is supposed that the relaxation process is conditioned by the entropy increase that arises due to the mixing of untransformed and transformed domains of the material (untransformed domains are any microinhomogeneities of the material: crazes, submicropores, some breaks of packing's compactness, etc.; transformed domains are those sites of the material where the relaxation process is already over). The structure of microinhomogeneities changes during the deformation process, and as the sample is under constant deformation, inhomogeneities interact with one another, forming the nonrelaxing material. The essence of such an interaction is, e.g., the mixing of two (or more than two) inhomogeneities and their conversion to the nonrelaxing material. Such a mechanism of the relaxation process is confirmed experimentally by positron annihilation.[15] To make the entropy calculation possible, it is necessary for the relaxation process to come through consequent equilibrium states. Slow diffusion of the transformed domains, formed inside the material, may be the limiting stage in reaching the equilibrium state. Therefore, two memory functions are introduced. The first one $T_1(\tau)$ is based on the analysis of the untransformed domains' interaction kinetics, which may be a reversible or irreversible[16] reaction of the n-th order. The first memory function is given in eq. (3):

$$T_1(\tau) = -\frac{S_0 T_1^*(\tau)}{k_b m_1} \tag{3}$$

S_0 is the initial entropy of the system; m_1, the total quantity of transformed and untransformed domains per unit volume; k_b, Bolzman's constant; and $T_1^*(\tau)$, the variable part of the memory function described in eq. (4):

$$T_1^*(\tau) = \frac{1}{[f_1(\tau) - \alpha_0]\ln[f_1(\tau) - \alpha_0] + [1 - f_1(\tau) + \alpha_0]\ln[1 - f_1(\tau) + \alpha_0]} + \frac{1}{\ln 2} \tag{4}$$

where $f_1(\tau) = 1/(1 + k^*\tau/\beta)^\beta$; k^* is the untransformed domains' interaction rate constant; $\beta = 1/(n - 1)$, where n is the order of untransformed domains' interaction reaction; α_0, part of transformed domains formed up to the end of deformation process; and τ, the time. Here, the function $f_1(\tau)$ has physical meaning only when $f_1(\tau) > 0.5$.

The second memory function that is based on microinhomogeneities diffusion kinetics is given in eq. (5):

$$T_2(\tau) = -\frac{S_0 T_2^*(\tau)}{k_b m_2} \tag{5}$$

where $m_2 = m_2^* \int_0^\infty T_2^*(\tau)\, d\tau$, m_2^* being the number of diffusing inhomogeneities and $T_2^*(\tau)$ is the variable part of memory function that is given in eq. (6):

$$T_2^*(\tau) = \frac{1}{f_2(\tau)\ln f_2(\tau) + [1 - f_2(\tau)]\ln[1 - f_2(\tau)]} + \frac{1}{\ln 2} \tag{6}$$

where $f_2(\tau) = a\tau^\gamma$, a and γ being the material's constants, which characterize the rate of diffusion (a) and the constraint's influence (γ).

Thus, if the inhomogeneities interaction kinetics is the limiting stage of the relaxation process, the first memory function holds good, and if diffusion is the limiting stage, this process can be described by the second memory function.

The stress-relaxation curves' approximation is carried out using Boltzman's equation:

$$\sigma(t) = \sigma_0 - \sigma_0 \frac{S_0}{k_b m_1} \int_0^t T_1^*(\tau)\, d\tau$$

$$\sigma(t) = \sigma_0 - \sigma_0 \frac{S_0}{k_b m_2} \int_0^t T_2^*(\tau)\, d\tau$$

The calculations for the integral values of $\int_0^t T_1^*(\tau)\, d\tau$ and $\int_0^t T_2^*(\tau)\, d\tau$ were taken from the literature.[16]

The results of our calculations for samples containing structures (**I**) and (**III**) with a rubber phase content of 28% and 43% by weight are presented in Table III. It is evident from the table that in both memory functions the correlation coefficient "r" is very high (it is very close to 1). The memory function $T_1(\tau)$ is more suitable for glassy polymers.[14,16] Hence, it can be assumed that the limiting stage of the relaxation process in glassy polymers is the inhomogeneities interaction kinetics. For the samples under consideration, it is found that r values for the memory function $T_1(\tau)$ is higher (Table II), though in many cases the difference of r for $T_1(\tau)$ and $T_2(\tau)$ is negligible. Thus, in general, the inhomogeneities interaction kinetics is the limiting stage of the relax-

Table III Memory Function Parameters Calculated from the Results of Stress Relaxation Curves Approximation

Temperature (°C)	$T_1(\tau)$ r	σ_0 (MPa)	σ_∞ (MPa)	k^* (min)	n	$\frac{m_1 k_b}{S_0}$	$\frac{m_1^* k_b}{S_0}$ (min^{-1})	$T_2(\tau)$ r	σ_0 (MPa)	σ_∞ (MPa)	γ	α	$\frac{m_2 k_b}{S_0}$	$\frac{m_2^* k_b}{S_0}$ (min^{-1})
Composition with structures (I) and (III), containing ~ 28 wt % of the rubbery phase														
20	.996	26.6	17.4	.001	4.33	6711	2.89	.994	22.8	19.5	.5	.05	245	7.0
50	.997	25.9	17.3	.01	2.67	654	3.03	.986	20.7	17.2	.5	.05	206	5.9
80	.998	22.5	15.0	.01	3.50	671	3.01	.989	18.2	15.1	.5	.05	204	5.8
110	.993	25.4	13.4	.01	4.33	493	2.12	.993	18.8	13.7	.5	.05	130	3.7
140	.997	18.9	7.7	.001	2.67	3636	1.69	.999	4.0	9.7	.5	.05	115	3.3
170	.992	22.1	9.1	.01	4.33	394	1.70	.989	14.9	9.4	.5	.05	95	2.7
200	.998	22.3	5.7	.01	4.33	311	1.34	.993	13.1	6.1	.5	.05	65	1.9
240	.998	19.7	2.7	.01	3.50	258	1.16	.988	9.8	2.8	.5	.05	49	1.4
270	.998	12.4	0.1	.01	2.43	216	1.00	.974	4.8	0	.5	.05	34	1.0
Composition with structures (I) and (III), containing ~ 43 wt % of rubbery phase														
20	.996	11.8	8.0	.01	6.00	709	3.06	.993	9.7	7.9	.5	.05	191	5.48
50	.98	11.7	6.3	.001	2.67	4717	2.19	.996	9.3	7.3	.4	.05	162	4.65
80	.996	7.4	4.0	.01	6.00	571	2.21	.994	5.8	4.4	.5	.05	146	4.18
110	.988	6.4	2.1	.001	6.00	3861	1.50	.985	4.8	3.3	.5	.0403	176	3.29
140	.995	7.4	1.7	.001	6.00	3344	1.30	.996	5.2	5.2	.5	.0403	144	2.70
170	.993	8.1	0	.001	6.00	2512	0.97	.997	4.9	4.9	.5	.0403	93	1.73
200	.994	6.5	0	.01	6.00	251	0.97	.989	3.2	3.2	.5	.05	41	1.18

ation process for these materials but at the same time the diffusion mechanism is also important.

The value of $(m_1^* k_b/S_0)$ that characterizes the number of inhomogeneities in the sample, for the composition of networks (I) and (II), containing 28% by weight of the rubbery phase does not change significantly from 295 to 350 K [Fig. 7(a), curve 1], but after 350 K, it decreases with increasing temperature. With an increasing rubbery phase content to 43% by weight [Fig. 7(a), curve 2], the initial region with a constant $(m_1^* k_b/S_0)$ value disappears, but it decreases slightly; $(m_1^* k_b/S_0)$ values are close for both the compositions.

The most important characteristic of polymeric materials is quasi-equilibrium stress, which can be calculated from the following equations:

$$\sigma_\infty = \sigma_0 - \sigma_0 \frac{S_0}{k_b m_1} \int_0^\infty T_1^*(\tau)\, d\tau$$

$$\sigma_\infty = \sigma_0 - \sigma_0 \frac{S_0}{k_b m_2} \int_0^\infty T_2^*(\tau)\, d\tau$$

These parameters are the results of stress-relaxation curve extrapolation to $t \to \infty$. σ_∞ decreases smoothly by six times with the growth of temperature from 295 to 510 K [Fig. 7(b), curves 4 and 5]. So, the quasi-equilibrium modulus E_∞ ($E_\infty = \sigma_\infty/\varepsilon_0$, where ε_0 is the final deformation), also decreases the same way. Generally, in the usual transition zone from the glassy to the rubbery state, the elasticity modulus decreases to several decimal orders. Hence, we can observe in the present case that there exists a wide temperature region where our networks with different compositions behave as the glassy polymers but at the same time have a modulus that is significantly lower than for the usual polymeric glasses. Only at the temperature of about 540 K is the quasi-equilibrium modulus is close to zero (Fig. 7, curves 4 and 5) and this is the glass transition of the rigid phase formed by the network. This value is close to the theoretical value (T_g) of the network with structure (I).

With an increasing rubbery phase content, the quasi-equilibrium modulus of the composition decreases [Fig. 7(b), curves 7 and 8). The temperature dependence of both of the modulii (initial and quasi-equilibrium) also changes its form. For the composition with the high rubbery content, both modulii are almost independent of the temperature in the region of 310–440 K [Fig. 7(b), curves 6–8]. So, here, we propose that for the high rubbery content com-

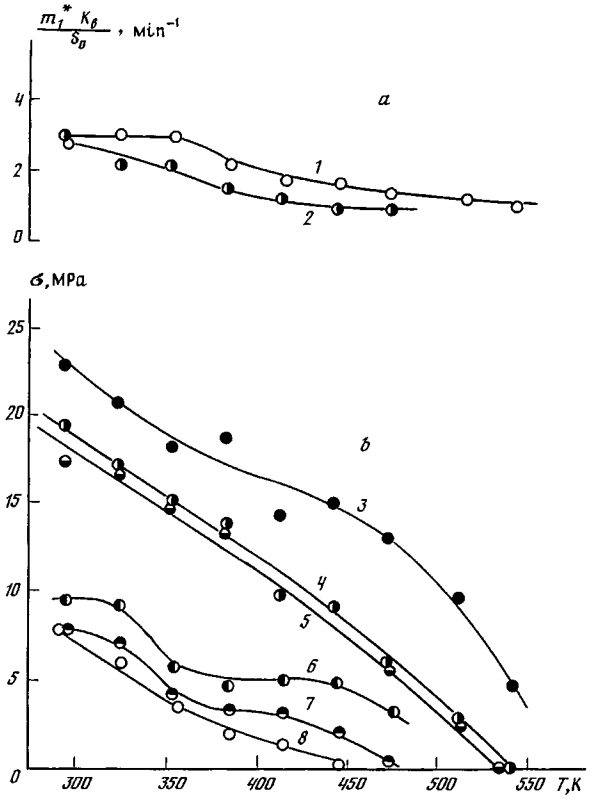

Figure 7 Relaxation parameter temperature dependence for the compositions with structures (**I**) and (**III**), containing (1, 3, 4, 5) ~ 28 and (2, 6, 7, 8) ~ 43 wt % of the rubbery phase. (a) $m_1^* k_b/S_0$ calculated by means of $T_1(\tau)$ memory function; (b) (3, 6) initial modulus, calculated by means of $T_2(\tau)$ memory function, and quasi-equilibrium modulus, calculated by means of (5, 8) $T_1(\tau)$ and (4, 7) $T_2(\tau)$ memory functions.

position the rise of the modulus of the rubbery network with increasing temperature superposes on the decrease of the modulus of the glassy network and as a result the changes in total modulus values are small.

It can also be noted that γ in $T_2(\tau)$ is equal to 0.5 for all the samples in the entire temperature region investigated. So, the microheterogeneities diffuse during the relaxation process in accordance with Fick's law.

CONCLUSIONS

Thus, the DMA data, structural investigations, and the stress-relaxation experiments show the unusual behavior of the synthesized network compositions. These compositions result in formation of heterophase systems of two types of morphology that have two or three relaxation transitions. The relaxation transitions at low and high temperatures correspond to the glass transitions of the rubbery phase and rigid network, respectively. If the components are semicompatible, then a third transition (between the above two temperatures) corresponding to the interphase is observed.

For both incompatible and semicompatible compositions, there is a possibility to vary the phase dimensions and so obtain the transparent samples having mechanical properties that differ from mechanical properties of both the glassy and rubbery polymers. These materials have an elasticity modulus, which is usual for the transition zone between the glassy and rubbery states, but its behavior is not viscoelastic; it is the same as for polymeric glasses. One can observe such a behavior in the wide temperature region between two transitions mentioned above. E' decreases smoothly after the first transition and the rate of this decrease is a little bit higher than that for usual polymeric glasses, but significantly lower than that for polymers in the transition zone. In the last case, the modulus decreases to several decimal orders in a very narrow temperature interval (20–30°C); however, for the materials investigated, the modulus decreases not more than 10 times and this decrease occurs in a wide temperature interval from 200 K to more than 500 K. In this case, this intermediate region between two transitions is the general field of application due to its great extent, and, here, we really have the new state of the polymer, which differs both from glassy and rubbery states. The difference is that these compositions have an intermediate elasticity modulus value, but also have elastic properties, similar to the polymer before and after the transition. Such unusual properties make it possible to use these materials in those fields of applications where the materials should be elastic with slight rigidity.

One of the authors (A. V. R.) wishes to express his sincere thanks to the University Grants Commission of India and the Russian Academy of Sciences for making this work possible under the Indo-Russian Cultural Exchange Programme.

REFERENCES

1. B. A. Rosenberg and E. F. Oleinik, *Uspekhi Khim.*, **53**, 273 (1984).
2. V. P. Volkov, G. G. Alexanian, A. A. Berlin, and B. A. Rosenberg, *Vysokomolek. Soedin. Ser. A*, **27**, 756 (1985).

3. A. A. Berlin, B. A. Rosenberg, and N. S. Enikolopian, *Dokl. AN SSSR,* **303,** 645 (1989).
4. A. J. Kinloch, S. J. Shaw, and D. L. Hunston, *Polymer,* **24,** 1341 (1983).
5. A. J. Kinloch and D. L. Hunston, *J. Mater. Sci. Lett.,* **6,** 137 (1987).
6. S. Numata and N. Kinjo, *Polym. J.,* **8,** 671 (1982).
7. A. A. Askadskii, G. V. Surov, V. A. Pankratov, Ts. M. Frenkel, L. I. Makarova, A. A. Zdanov, I. V. Blagodatskyh, and A. V. Pastukhov, *Vysokomolek. Soedin. Ser. A,* **32,** 1528 (1990); *Chem. Abstr.,* **113**(14), 116413t (1990).
8. A. A. Askadskii, Yu. I. Matveev, F. N. Nurmukhametov, G. L. Slonimskii, and B. D. Tartakovskii, *Mekhan. Polim.,* **2,** 340 (1975).
9. A. A. Askadskii, in *Polymer Yearbook, No 4,* R. A. Pethrick Ed., Harwood Academic Publishers, Chur, London, Paris, New York, Melbourne, 1987, p. 93.
10. A. A. Askadskii, Yu. I. Matveev, A. V. Pastukhov, B. A. Rosenberg, T. I. Ponomareva, N. A. Tschegolevskaya, and A. S. Martschalkovitsch, *Vysokomolek. Soedin. Ser. A,* **25,** 56 (1983); *Chem. Abstr.,* **98**(16), 126916v (1983).
11. A. A. Askadskii, V. A. Pankratov, Ts. M. Frenkel, A. E. Schvorak, T. M. Babtschinitzer, O. V. Kovriga, and C. A. Bychko, *Vysokomolek. Soedin. Ser. A.,* **32,** 2129 (1990).
12. T. M. Babtschinitzer, Ya. V. Genin, A. R. Korigodsky, M. D. Afaunov, D. F. Kutepov, and V. V. Korshak, *Polym. Commun.,* **25**(10), 229 (1984).
13. V. R. Regel, G. V. Berejkova, and G. A. Dubov, *Zavodskaya Lab.,* **25,** 101 (1959).
14. A. A. Askadskii, *Mekhan. Kompos. Mater.,* **3,** 403 (1987).
15. A. A. Askadskii, S. A. Tishin, V. V. Kazantseva, and O. V. Kovriga, *Vysokomolek. Soedin. Ser. A,* **32,** 2437 (1990); *Chem. Abstr.,* **114**(24), 229821p (1991).
16. A. A. Askadskii, A. L. Blumenfeld, E. G. Galpern, and A. L. Tschystyakov, *Vysokomolek. Soedin. Ser. A,* **30,** 886 (1988); *Chem. Abstr.,* **108**(24), 205476e (1988).

Received December 11, 1993
Accepted August 30, 1994